4th International Conference on
Earthquake Geotechnical Engineering
June 25-28, 2007
Paper No. 1242

A DIAGONAL CONSISTENT MASS MATRIX FOR EARTHQUAKE SITE RESPONSE SIMULATIONS

Evelyne FOERSTER[1], Hormoz MODARESSI[2]

ABSTRACT

Computational aspects and especially mass matrix determination, play a key part in soil dynamics applications. In seismic response analyses of soils, one option is to perform finite-element transient analyses on one-dimensional multi-layered profiles assuming various initial and boundary conditions. Diagonal mass matrices are generally preferred with explicit integration schemes, as no inversion of the overall system matrix is required at each time-step, thus reducing computation costs. One of the widely used methods to diagonalize a consistent matrix is the lumping scheme. Another method can be envisaged in case of isoparametric finite elements, without using the lumping scheme, and which is based on the enrichment of the shape functions and the selection of the appropriate integration order. In this paper, we present this scheme (so called the "diagonal consistent" scheme) we have adapted for 1D isoparametric quadratic finite elements. Then, we analyse the stability requirements for the 1D seismic analysis when considering explicit and implicit-explicit integration schemes, as well as various initial and boundary conditions. Through numerical applications, we also show the advantages to use the proposed diagonal mass matrix over a classical lumped mass matrix.

Keywords: Diagonal Consistent Mass matrix, FEM modelling, Stability analysis, Soil dynamics

INTRODUCTION

Computational aspects and especially mass matrix determination, play a key role in soil dynamics or classical mechanics applications. In seismic response analyses of soils, a one-dimensional multi-layered geometry is usually assumed with homogeneous laterally semi-infinite layers overlying a rigid or a deformable elastic bedrock. This one-dimensional geometry remains valid when no lateral heterogeneity, either geometric or material, does exist. Two numerical approaches can be considered for analysis: either a linear equivalent approach performed in the frequency domain (Idriss & Seed 1968; Seed & Idriss, 1970), or a finite-element (FEM) transient approach for porous media, in which a water table can be considered, assuming various hydraulic conditions within the soil profile, such as the total drainage for layers above the water table, and totally undrained or partially drained (so called coupled two-phase approach) for saturated layers underneath.

When performing FEM analyses with non linear constitutive modelling, implicit numerical integration schemes are generally preferred as they lead to unconditional stability. However, they require an iterative scheme and the inversion of a consistent matrix solver at each time-step, which can be a memory and also time consuming process. On the contrary, diagonal mass matrices are generally best fit for explicit schemes, preferably with linear analysis, as no inversion of the overall system matrix is

[1] Research Project Leader, Development Planning and Natural Risks Department, French Geological Survey (BRGM), France, Email: e.foerster@brgm.fr
[2] Professor, Head of the Development Planning and Natural Risks Department, French Geological Survey (BRGM), France.

required at each time-step, thus reducing computation costs. However, they require very small computation steps to fulfil numerical stability conditions.

Different schemes exist to diagonalize a consistent matrix, and the lumping scheme is certainly one of the simplest and widely used methods (Zienkiewicz and Taylor, 1991). The lumping process can be achieved for instance, by using the diagonal terms of the consistent matrix and form a diagonal matrix by scaling these entries so that the total mass of the element is conserved. In this paper, we present another method, the "diagonal consistent scheme", which is based on the enrichment of the shape functions and the selection of the appropriate integration order. This method was originally proposed by Sauer (1993) for isoparametric linear quadrilateral (2D) and hexahedron (3D) finite elements and we have adapted it for 1D isoparametric quadratic finite elements.

In next sections, we first recall the governing equations and numerical implementation of the 1D multi-kinematics model we use for earthquake site response analysis and we present the method to obtain a "diagonal consistent" mass matrix which is used in the seismic analysis. Then, we analyse the stability requirements for two integration schemes, when considering two boundary conditions at the base of the soil profile, namely the rigid bedrock and the deformable bedrock conditions. Finally, we present numerical applications putting emphasis on the stability conditions and also on the advantages to use a consistent diagonal mass matrix, instead of a classical lumped mass matrix.

PRESENTATION OF THE 1D MULTI-KINEMATICS MODEL FOR EARTHQUAKE SITE RESPONSE ANALYSIS

General assumptions

The one-dimensional model used in this paper for seismic analysis considers a soil profile modeled as a multi-layered dry or saturated porous medium with homogeneous laterally semi-infinite layers lying over a rigid or elastic bedrock (Fig. 1). This 1D geometry remains valid when no lateral heterogeneity, either geometric or material, does exist. The model kinematics is three-dimensional, with two horizontal and one vertical components of motion. When a water table is present in the soil profile, layers located above the water level are assumed to be totally drained, whereas the saturated layers underneath are considered as fully undrained or partially drained (coupled two-phase analysis).

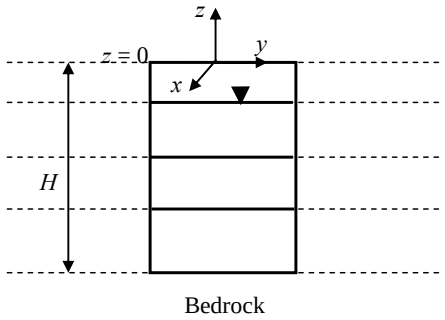

Figure 1. 1D multi-layered soil profile used for seismic analysis

In this model, a transient analysis is performed, which is based on the resolution of the simplified *u-p* Biot's macroscopic dynamic model (Zienkiewicz *et al.*, 1980), and which is obtained by combining the momentum conservation law with the mass conservation equation for fluid and solid phases, together with a generalized Darcy's law for fluid flow through the porous medium and Terzaghi's effective stress principle. As for the main assumptions, we consider that: (i) the fluid relative acceleration can be neglected before the solid skeleton acceleration for low frequency loadings (generally verified in the seismic case); (ii) the fluid is incompressible and the solid phase is homogeneous, isotropic and incompressible; (iii) the permeability is independent of the frequency; and (iv) physico-chemical interactions as well as thermal effects can be neglected. Moreover, the initial conditions are derived from the initial static state, that is the hydrostatic pressure and initial static

stresses due to self weight and slope, prevailing before the seismic motion. Finally, if a water table is present, the bedrock is assumed to be impervious so that no flux occurs across the interface boundary between the studied domain and the underlying semi-infinite space.

In the following formulation, we consider the (*xyz*) coordinates as the principal directions for strain/stress analysis, with normal effective stress along the *z*-axis and shearing in the *x*-*z* and *y*-*z* planes. Moreover, a '*z*' subscript indicates a vector component along the *z*-axis and an underline quantity means a horizontal vector - components along *x* and *y* axes-.

Governing equations

The governing equations are expressed in the (*xyz*) coordinates as follows:

$$\rho \partial_t v_i = \partial_z \tau_{iz} \qquad i \in \{x, y\} \tag{1}$$

$$\begin{cases} \rho \partial_t v_z + \partial_z p = \partial_z \sigma' \\ \partial_z v_z - k \partial_{zz} p = 0 \end{cases} \tag{2}$$

where τ_{iz} and σ' represent the dynamic shear and normal effective stresses respectively, i.e. the increments of stresses with respect to the initial static state; p is the excess pore-water pressure; v_i and v_z are the horizontal and vertical components of the absolute skeleton velocity field; ρ is the saturated mass density of soil materials, and finally, ∂_z and ∂_{zz} are the partial first- and second-order derivatives with respect to *z* direction.

Eq. (1) is related to the horizontal motion of the soil profile and system (2) applies for layers located underneath the water table position, considering a partially draining condition. These equations are general and applies for any draining condition. For instance, when dealing with layers above the water table, it can be simplified as the terms associated to the fluid flow disappear.

The seismic input motion is prescribed at the bottom of the studied soil profile, namely at the interface Σ between soil layers and the bedrock. When the contrast of impedance between the underlying bedrock and the soil profile is high enough to assume the bedrock as rigid, the studied domain can be limited to the deformable soils. The rigid bedrock condition leads to prescribe a null relative motion at the bottom of the soil profile.

When the bedrock can not be assumed as rigid, its deformability and the transient evolution of the seismic field have to be taken into account. A zeroth-order paraxial approximation is used in the model as a local absorbing boundary condition, which permits diffracting waves to be evacuated from the study domain, but also permits to introduce the incident field in the study domain (Modaressi and Benzenati, 1994).

Numerical implementation

Hreafter, we present the numerical integration of the weak formulation obtained from the governing equations (1) and (2) and following the virtual work principle over the studied domain, in the linear elasticity framework. Spatial integration is performed using 1D isoparametric finite elements and nodal quadrature. As the fluid phase is incompressible, two different spaces are used to prevent locking of the finite-element mesh and spurious oscillations in the pore-pressure field for low permeability values (Zienkiewicz and Taylor, 1991). Thus, a quadratic interpolation is used for the velocity fields and a linear interpolation is used for the excess pore-pressure field.
Moreover, explicit and implicit-explicit predictor-corrector Newmark schemes are adopted for the integration with respect to time.

Displacement, velocity and pore-pressure fields are predicted at time $t = t_{n+1}$ as:

$$\begin{cases} \tilde{u}_{n+1} = u_n + \Delta t\, v_n + \left(\frac{1}{2} - \beta\right)\Delta t^2 \dot{v}_n \quad \text{and } \tilde{v}_{n+1} = v_n + (1-\gamma)\Delta t\, \dot{v}_n \\ \tilde{p}_{n+1} = p_n + (1-\theta)\Delta t\, \dot{p}_n \end{cases} \tag{3}$$

noting predicted value of variable x at t_{n+1} as $\tilde{x}_{n+1}$.

In the correction phase, all fields are evaluated as:

$$\begin{cases} u_{n+1} = \tilde{u}_{n+1} + \beta\, \Delta t^2 \dot{v}_{n+1} \text{ and } \; v_{n+1} = \tilde{v}_{n+1} + \gamma\, \Delta t\, \dot{v}_{n+1} \\ p_{n+1} = \tilde{p}_{n+1} + \theta\, \Delta t\, \dot{p}_{n+1} \end{cases} \tag{4}$$

The final discretized system for the finite-element mesh at time t_{n+1} is expressed as follows:

$$\boldsymbol{M}\, \dot{\boldsymbol{V}}_{n+1} = -\boldsymbol{K}\tilde{\boldsymbol{U}}_{n+1} + \delta_b \underbrace{\boldsymbol{M}_b \left(2\boldsymbol{V}^i_{n+1} - \tilde{\boldsymbol{V}}_{p,n+1}\right)}_{\boldsymbol{T}_b} \tag{5}$$

$$\begin{cases} \boldsymbol{M}\, \dot{\boldsymbol{V}}_{z,n+1} - \boldsymbol{L}\boldsymbol{P}_{n+1} = -\boldsymbol{K}\tilde{\boldsymbol{U}}_{z,n+1} + \delta_b \underbrace{\boldsymbol{M}_{bz} \left(2\boldsymbol{V}^i_{z,n+1} - \tilde{\boldsymbol{V}}_{pz,n+1}\right)}_{\boldsymbol{T}_{bz}} \\ -\boldsymbol{L}^T \dot{\boldsymbol{V}}_{z,n+1} - \dfrac{\boldsymbol{H}}{\gamma \Delta t} \boldsymbol{P}_{n+1} = \dfrac{\boldsymbol{L}^T}{\gamma \Delta t} \tilde{\boldsymbol{V}}_{z,n+1} \end{cases} \tag{6}$$

with:

- $\boldsymbol{M}$, $\boldsymbol{K}$, $\boldsymbol{H}$, $\boldsymbol{L}$: mass, rigidity, permeability and coupling operators;
- $\{\dot{\boldsymbol{V}}, \dot{\boldsymbol{V}}_z\}$, $\boldsymbol{P}$: unknown vectors of nodal accelerations and excess pore-pressures;
- $\{\tilde{\boldsymbol{V}}, \tilde{\boldsymbol{V}}_z\}$: vectors of predicted nodal velocities;
- $\{\tilde{\boldsymbol{U}}, \tilde{\boldsymbol{U}}_z\}$: vectors of predicted nodal displacements;
- δ_b : numerical coefficient set to one for the element at the bottom of the soil column in case of a deformable bedrock condition, else $\delta_b = 0$.
- $\{\boldsymbol{T}_b, \boldsymbol{T}_{bz}\}$: total nodal stress vector to be evaluated over the deformable bedrock boundary Σ, and which represents the transient action exerted by the outer semi-infinite domain on the bounded inner domain (soil column). In this case, $\{\boldsymbol{V}^i, \boldsymbol{V}^i_z\}$ represent the vectors of nodal incident wave velocities and $\{\tilde{\boldsymbol{V}}_p, \tilde{\boldsymbol{V}}_{pz}\}$, the vectors of predicted velocities at node on Σ.

In absence of water and assuming a linear elastic behavior for materials in the vicinity of Σ, the $\{\boldsymbol{M}_b, \boldsymbol{M}_{bz}\}$ terms can be expressed as:

$$\begin{bmatrix} \boldsymbol{M}_b \\ \boldsymbol{M}_{bz} \end{bmatrix}_{IJ} = \delta_{I2}\delta_{IJ} \begin{bmatrix} \rho\, c_s \\ \rho\, c_p \end{bmatrix} \tag{7}$$

with nodes (I, J) $\{1, 3\}^2$, and δ_{IJ} , the Kroenecker symbol.

System of equations (5) and (6) is general and can be used for various conditions (rigid/deformable bedrock, water/no water).

Implementation of the "diagonal consistent" mass matrix for 1D quadratic finite element

In the "diagonal consistent" scheme, we modify the standard 1D quadratic shape functions by introducing two independent real parameters α_1 and α_2, in order to obtain expansion to a higher order:

$$\forall r \in [-1,1], \begin{cases} N_1(r,\alpha_1,\alpha_2) = \frac{1}{2} r\left[(1-\alpha_2)r - (1-\alpha_1) - \alpha_1 r^2 + \alpha_2 r^3\right] \\ N_2(r,\alpha_1,\alpha_2) = \frac{1}{2} r\left[(1-\alpha_2)r + (1-\alpha_1) + \alpha_1 r^2 + \alpha_2 r^3\right] \\ N_3(r,\alpha_2) = 1 - (1-\alpha_2)r^2 - \alpha_2 r^4 \qquad \text{(middle node)} \end{cases} \tag{8}$$

where N_I is the quadratic shape function at node I and r, the reference coordinate of the element (Fig. 2). We note here that setting α_1 and α_2 to zero gives the standard shape functions leading to the usual consistent mass matrix.

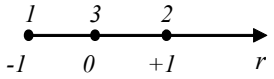

Figure 2. Reference coordinate for the 1D quadratic finite element

The components M_{IJ} of the new mass matrix are then derived from the following relation:

$$\forall I \neq J,\ M_{IJ}^{e}(\alpha_1,\alpha_2) = \rho \frac{\Delta z}{2} \int_{\Omega^e} N_I(r,\alpha_1,\alpha_2) N_J(r,\alpha_1,\alpha_2)\, dr \tag{9}$$

with Δz, the quadratic element size.

The new mass matrix terms being expressed as a function of α_1 and α_2 parameters, we then diagonalize the matrix by finding α_1 and α_2, so that off-diagonal terms be zero. This gives the following values for α_1 and α_2:

$$\alpha_1 = \left(14 \pm \sqrt{238 + 14\sqrt{345}}\right) \Big/ 8 \text{ and } \alpha_2 = -\left(3 + \sqrt{345}\right) \Big/ 8 \tag{10}$$

With values (10), the diagonal terms of the new mass matrix are given as:

$$M_{11} = M_{22} = \rho \frac{\Delta z}{120}\left(23 + \sqrt{345}\right) \text{ and } M_{33} = \rho \frac{\Delta z}{60}\left(37 - \sqrt{345}\right) \tag{11}$$

STABILITY ANALYSIS

For each scheme, we consider the element-by-element free vibration motion (linear elasticity) and we solve the generalized eigenvalue problem at time $t_{n+1} = (n+1)\Delta t$, seeking for non trivial solution of the form:

$$\boldsymbol{U}_{n+1} = e^{i\omega\Delta t} \underbrace{\left[\bar{\boldsymbol{U}}\, e^{i\omega n\Delta t}\right]}_{\boldsymbol{U}_n} = \lambda \boldsymbol{U}_n \tag{12}$$

with ω, the free vibration frequency and $\bar{\boldsymbol{U}}$, the corresponding free vibration mode.

Then stability requires that there be no amplification of the solution (Park, 1983):

$$\left\| \frac{\boldsymbol{U}_{n+1}}{\boldsymbol{U}_n} \right\| = |\lambda| \le 1 \tag{13}$$

Writing the free vibration condition for equations (5) and (6) gives:

$$\boldsymbol{M}\,\dot{\boldsymbol{V}}_{n+1} = -\boldsymbol{K}\tilde{\boldsymbol{U}}_{n+1} - \delta_b\,\boldsymbol{M}_b\,\tilde{\boldsymbol{V}}_{p,n+1} \tag{14}$$

$$\begin{cases} \boldsymbol{M}\,\dot{\boldsymbol{V}}_{z,n+1} - \boldsymbol{L}\boldsymbol{P}_{n+1} = -\boldsymbol{K}\tilde{\boldsymbol{U}}_{z,n+1} - \delta_b\,\boldsymbol{M}_{bz}\,\tilde{\boldsymbol{V}}_{pz,n+1} \\ -\boldsymbol{L}^T\,\dot{\boldsymbol{V}}_{z,n+1} - \dfrac{\boldsymbol{H}}{\gamma\Delta t}\,\boldsymbol{P}_{n+1} = \dfrac{\boldsymbol{L}^T}{\gamma\Delta t}\tilde{\boldsymbol{V}}_{z,n+1} \end{cases} \tag{15}$$

Then, in order to find the elementary generalized eigenvalue problems corresponding to equations (14) and (15), we need to express $\tilde{\boldsymbol{U}}_{n+1}$ and $\tilde{\boldsymbol{V}}_{n+1}$ versus $\boldsymbol{U}_{n+1}$, using Newmark scheme (4), which gives:

$$\tilde{\boldsymbol{U}}_{n+1} = \left(1 + \beta\omega^2\Delta t^2\right)\boldsymbol{U}_{n+1} \quad \text{and} \quad \tilde{\boldsymbol{V}}_{n+1} = \left(i\omega + \gamma\omega^2\Delta t\right)\boldsymbol{U}_{n+1} \tag{16}$$

Combining (14), (15) and (16) leads to the following elementary generalized eigenvalue problems:

$$\left[\boldsymbol{K} - \omega^2\left(\boldsymbol{M} - \beta\,\Delta t^2\,\boldsymbol{K} - \gamma\,\Delta t\,\delta_b\boldsymbol{M}_b\right) + i\omega\,\delta_b\boldsymbol{M}_b\right]\boldsymbol{U}_{n+1} = \boldsymbol{0} \tag{17}$$

$$\begin{bmatrix} \boldsymbol{K} - \omega^2\left(\boldsymbol{M} - \beta\,\Delta t^2\,\boldsymbol{K} - \gamma\,\Delta t\,\delta_b\boldsymbol{M}_{bz}\right) + i\omega\,\delta_b\boldsymbol{M}_{bz} & -\boldsymbol{L} \\ -\boldsymbol{L}^T & \dfrac{i\boldsymbol{H}}{\omega} \end{bmatrix} \begin{bmatrix} \boldsymbol{U}_{z,n+1} \\ \boldsymbol{P}_{n+1} \end{bmatrix} = \boldsymbol{0} \tag{18}$$

Computing the roots of the characteristic polynomial for Eq. (17), considering a rigid or deformable bedrock, leads to the following critical time-step values for the explicit integration scheme:

$$\Delta t < \frac{\Delta z}{c_S}\sqrt{\frac{3AB}{8\beta}} = \Delta t^R_{crit} \qquad \text{with } \delta_b = 0 \tag{19}$$

$$\Delta t < \frac{\Delta z}{c_S}\sqrt{\frac{(7+2A) - \sqrt{(7+2A)^2 - 192AB}}{32\beta}} = \Delta t^D_{crit} \qquad \text{with } \delta_b = 1 \tag{20}$$

with $\{\, A = (23 + \sqrt{345})/120\,,\ B = (37 - \sqrt{345})/60\,\}$ for the "diagonal consistent" scheme, and $\{\, A = 1/6\,,\ B = 2/3\,\}$, for the lumped scheme.

Condition (20) being less restrictive on the time-step than (19), the critical time-step (19) is considered for stability requirements of the explicit integration scheme with a rigid or a deformable bedrock.

Determining the characteristic polynomial $\boldsymbol{P}_I(\omega)$ for Eq. (18) using *Mathematica*® software, and solving for $\boldsymbol{P}_I(\omega) = 0$ leads to real solutions for ω, for both bedrock conditions (rigid or deformable). So the implicit-explicit integration scheme is unconditionally stable.

Finally, the critical time-step Δt_{crit}^{R} computed in (19) is to be considered in the seismic analysis, whatever the bedrock and draining conditions.

NUMERICAL APPLICATIONS

Stability of the explicit scheme

The examples in this section show the numerical results obtained with a totally drained elastic soil profile subjected to a horizontal input motion in the form of a Ricker wavelet of order 2, and considering a rigid or deformable bedrock condition (Fig. 3). The time steps for analysis are chosen near the critical value (19) as determined to fulfill stability requirements of the explicit scheme. Values of A and B coefficients are those for a "diagonal consistent" mass matrix and the value of β coefficient is set equal to 0.25.

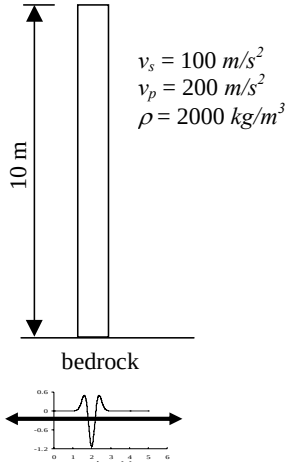

Figure 3. Elastic soil profile considered for stability analysis (no water)

In figures 4 and 5, we see that using a time-step slightly over the critical time-step either for a rigid or a deformable bedrock boundary condition, leads to strong numerical instabilities. When the time-step is equal to the critical one, spurious oscillations appear (Fig. 4).

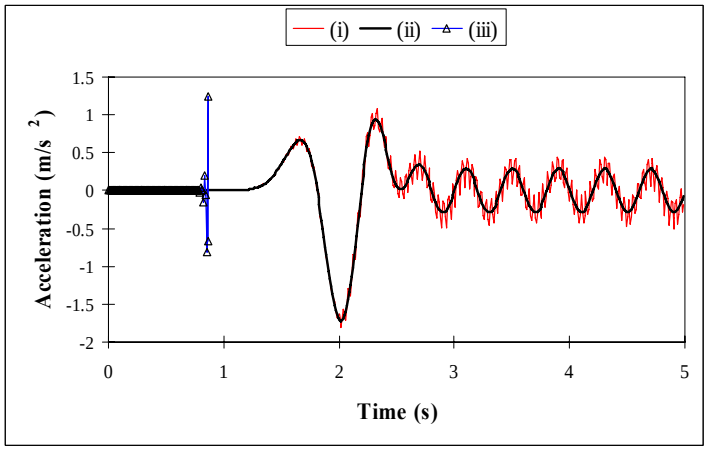

Figure 4. Horizontal accelerations computed at ground surface (rigid bedrock): (i) $\Delta t = \Delta t_{crit}^{R}$, (ii) $\Delta t = 0.9\Delta t_{crit}^{R}$ (stable), (iii) $\Delta t = 1.1\Delta t_{crit}^{R}$ (unstable).

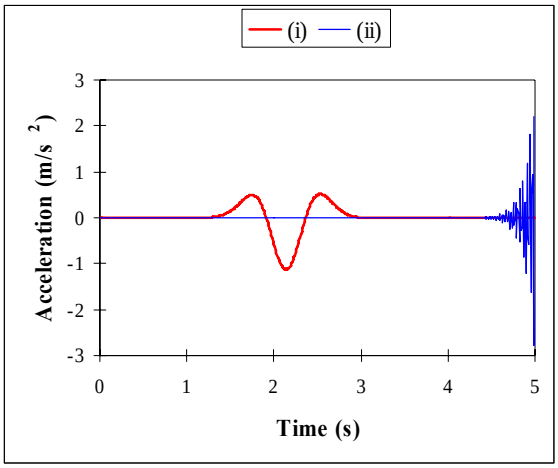

Figure 5. Horizontal accelerations computed at ground surface (deformable bedrock): (i) $\Delta t = 0.988\Delta t^R_{crit}$ (stable), (ii) $\Delta t = 1.007\Delta t^R_{crit}$ (unstable).

Comparison between the lumped and "diagonal consistent" mass matrix schemes

Two examples are chosen to compare the performance of the "diagonal consistent" and lumped mass matrices. Figure 6 shows the elastic soil profile subjected to a vertical harmonic input motion, which frequency of 1.25Hz corresponds to the fundamental frequency of the studied column. Value of β coefficient is set equal to 0.25 and time-step value for computations is equal to 0.003 seconds, which is under the critical time-step value ($\Delta t^R_{crit} = 0.004\,\text{sec}$ in this case).

When comparing the vertical accelerations obtained with both mass matrices to the closed-form response, in the case of a totally drained soil profile (no water), we see that the diagonal consistent mass matrix gives more accurate results than the lumped one (Fig. 7).

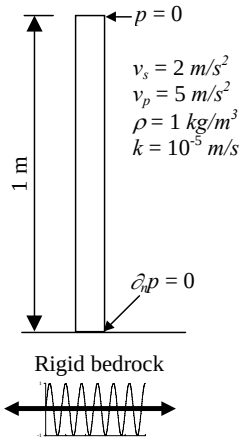

Figure 6. Elastic soil profile used for comparison of the lumped and "diagonal consistent" mass matrix schemes

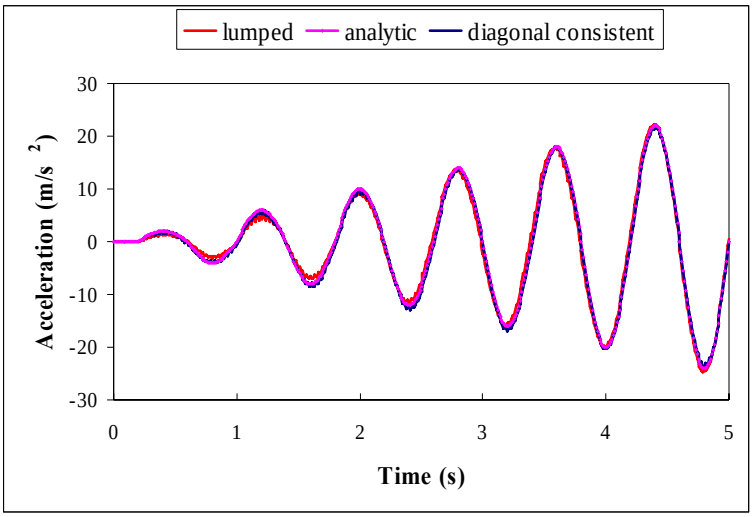

Figure 7. Accelerations computed at ground surface (rigid bedrock, no water): comparison between the analytical solution and lumped/diagonal consistent mass matrices.

When considering a coupled two-phase analysis for the soil profile, we note that the standard lumped mass matrix leads to spurious oscillations for the vertical motion computed at ground surface (Fig. 8), while the diagonal consistent mass gives smooth results. Using the lumped mass in this case induces more high frequencies in the soil response (Fig. 8), which is a purely numerical fact and would lead to numerous loading/unloading cycles if a non linear constitutive model was used. However, we note that the excess pore-pressure responses obtained with both mass matrices are very similar (Fig. 9).

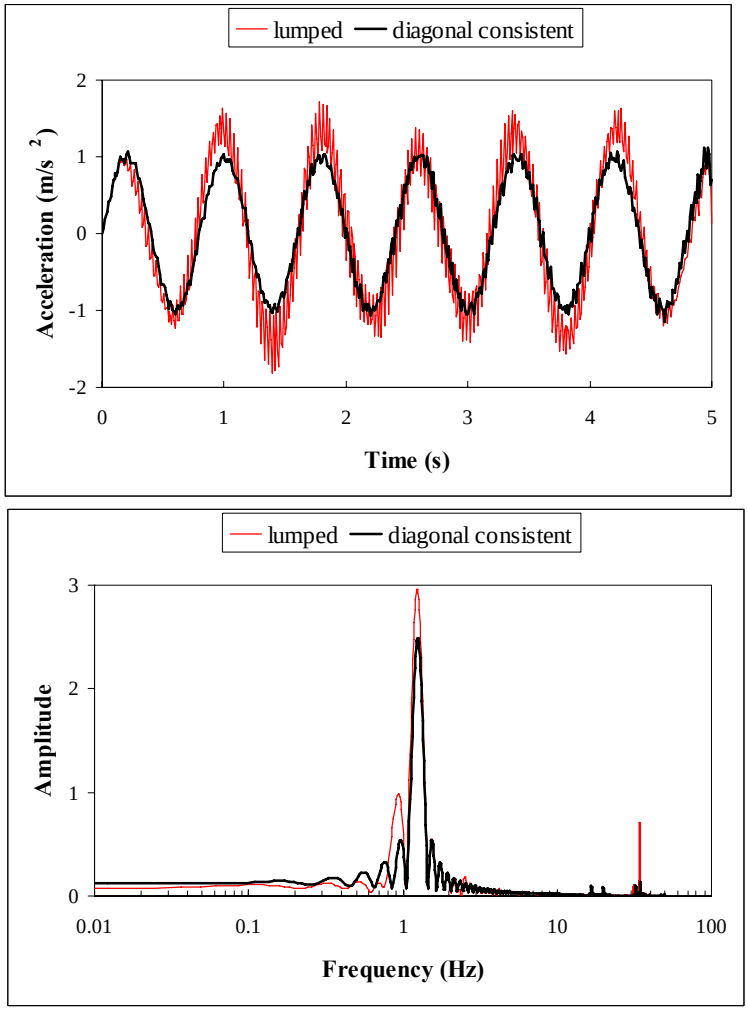

Figure 8. Accelerations and related spectral amplitudes at ground surface (rigid bedrock, two-phase analysis): comparison between the lumped/diagonal consistent mass matrices.

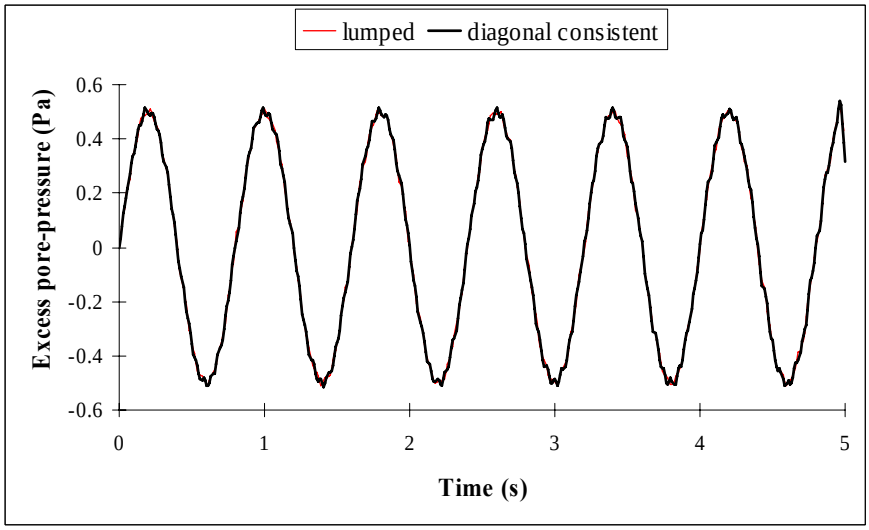

Figure 10. Excess pore-pressure obtained at mid-column with the rigid bedrock and partly drained conditions: comparison between the lumped/diagonal consistent mass matrix schemes.

CONCLUSIONS

In this paper, a 1D multi-kinematics model for earthquake site response analysis is presented, in which a “diagonal consistent” mass matrix scheme adapted for 1D isoparametric quadratic finite elements is implemented. The stability requirements are also examined and a critical time-step is given, which works for either the proposed explicit or implicit-explicit integration schemes, as well as for various initial and boundary conditions (rigid/deformable bedrock, water/no water). Through numerical applications, we demonstrate the numerical issues linked to stability condition violation and we show that in some cases, the standard lumped mass matrix leads to produce purely numerical higher frequencies, whereas the proposed diagonal mass matrix gives smoother results.

REFERENCES

Idriss IM and Seed HB. “Seismic response of horizontal soil layers,” Journal of the Soil and Mechanics Foundation Division, ASCE, 94, 1003-1031, 1968.

Modaressi H. and Benzenati I. “Paraxial approximation for poroelastic media,” Soil Dynamics and Earthquake Engineering, 13, 117-29,1994.

Park KC. “Stabilization of partitioned solution procedure for pore-fluid-soil interaction analysis,” Int. J. Num. Meth. Engrg., 19, 1669-73, 1983.

Sauer G. “Consistent diagonal mass matrices for the isoparametric 4-node quadrilateral and 8-node hexahedron elements,” Communications in Numerical Methods in Engineering, 9, Issue 1, 35-43, 1993.

Seed HB and Idriss IM. “Soil moduli and damping factors for dynamic response analysis of horizontally layered sites,” Report No. UCB/EERC-72/10. Earthquake Engineering Research Center, University of California, Berkeley. 1970.

Zienkiewicz OC, Chang CT and Bettess P. “Drained, undrained, consolidating and dynamic behaviour assumptions in soils,” Géotechnique, 30, Issue 4, 385-395, 1980.

Zienkiewicz OC and Taylor RL. “The Finite Element Method,” 4th ed., Vols. 1 and 2, McGraw-Hill, London, 1991.